Dear Andreas Richter,

We have studied comments carefully and made corrections, which we hope meet with approval. Comments and responses are listed as follows. In order to facilitate the reference to the questions and proposed changes, we use the following color coding:

Color coding:

Referee comment

Our answer

Proposed change in manuscript

As pointed out by one of the reviewers, there is a clear difference in the time constant of the SO2 and CO2 sensors. This is less visible in the revised manuscript as you changed the scale but this is something that you need to address. From what I see in your original graphs, the SO2 instrument has a much shorter time constant and thus shows more variability and a time shift compared the CO2 instrument. This is of course a problem when computing FSC if the measurement time in the centre of the plume is short. In such conditions, the SO2 peak will be larger than the corresponding peak in CO2 and the FSC will be overestimated. I think the proper approach would be to either take averages long enough to make sure that the full signal is taken by both instruments (30 seconds) or to numerically degrade the SO2 time series to correspond to the time constant of the CO2 instrument.

"take averages long enough to make sure that the full signal is taken by both instruments (30 seconds)". Indeed, this is a very important question. If the time is too long (30 s), it is difficult to ensure that all of the measurements in the integral interval are stable and undisturbed, especially for poor-quality data. In addition, the length of the valid data (especially for SO_2) may be less than 30 s. Take 2019-3-29A for example, part of original measurement data is as bellow:

Table 1 part of original measurement data of 2019-3-29A

Time	SO_2 (ppm)	CO_2 (ppm)	Time	SO_2 (ppm)	CO_2 (ppm)
10:38:09	0	3373	10:38:25	0.25	2504
10:38:10	0	3342	10:38:26	0.28	2636
10:38:11	0	3272	10:38:27	0.44	2813
10:38:12	0.18	3176	10:38:28	0.75	3287
10:38:13	0.06	3063	10:38:29	1.43	3558
10:38:14	0.17	2943	10:38:30	1.63	3822
10:38:15	0.37	2775	10:38:31	1.45	4074
10:38:16	0.19	2712	10:38:32	1.21	4290
10:38:17	0.37	2675	10:38:33	0.72	4417
10:38:18	0.16	2646	10:38:34	0.34	4622
10:38:19	0.1	2619	10:38:35	0.55	4662
10:38:20	0.29	2584	10:38:36	0.61	4671
10:38:21	0.46	2537	10:38:37	0.11	4660
10:38:22	0.51	2423	10:38:38	0.2	4622
10:38:23	0.41	2409	10:38:39	0	4560
10:38:24	0.44	2426	10:38:40	0	4469

"to numerically degrade the SO2 time series to correspond to the time constant of the CO2 instrument". A related question is, whether you have used exactly the same time for the readings of the maximum values of SO2 and CO2, although there is an obvious time shift between the two.

This is one approach that can be taken. Assume that the data in Table 1 are average data within 10s and can be used as the selection values for the FSC. There are three ways to select peak values:

Case 1: 1.63 for SO_2, 3822 for CO_2; The result value of FSC is relatively large.

Case 2: 0.61 for SO_2, 4671 for CO_2; The result value of FSC is relatively small.

Case 3: 1.63 for SO_2, 4671 for CO_2; The result value of FSC is relatively moderate.

What we did before was the option 1. The reason for this is that some of the sulfur is not converted to SO_2 (possibly SO_3 or SO_4). Choosing a larger result value may be closer to the true value.

In our first-generation pod (Zhou et al., 2019). Overall, despite the use of option 1, there was a high incidence of low estimates as shown in Figure 1.

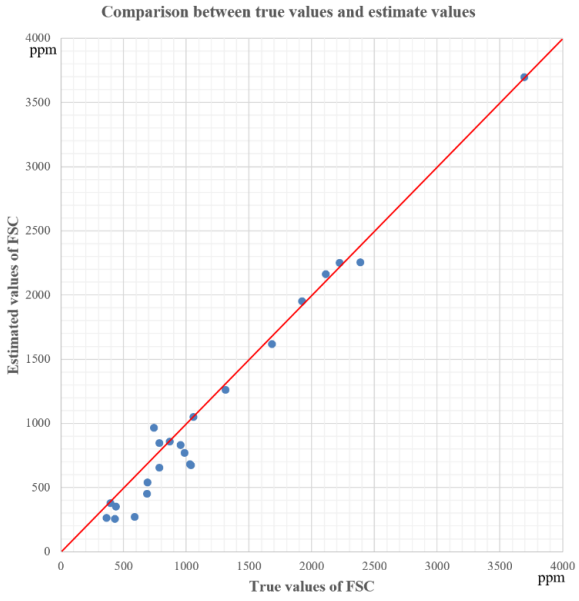

Figure 1. Comparison between the true values of FSC (x-axis) against the estimated values of FSC (y-axis) of 23 times measurement.

Therefore, the first-generation pod is suitable for adopting option 1 to obtain more accurate FSC.

It should be noted that the sensors of the first- and second-generation pod were provided by different manufacturer.

In our second-generation pod (this research), I also have done comparisons as listed below in Table 2. The deviation of results obtained in option 1 and 3 were similar on the whole. My initial choice is option 1, but option 3 is also OK.

Table 2 Comparison of option 1 and option 3

ID	Estimated FSC of option 3 (deviation)	Estimated FSC of option 1 (deviation)	True value of FSC
2019-3-18A	0.207 (-0.015)	0.217 (-0.005)	0.222
2019-3-22A	0.062 (-0.037)	0.069 (-0.030)	0.099
2019-3-22B	0.046 (0.004)	0.046 (0.004)	0.042
2019-3-29A	0.051 (0.016)	0.057 (0.022)	0.035
2019-4-1A	0.064 (-0.015)	0.090 (0.011)	0.079
2019-4-3A	<0.020	<0.020	0.013
2019-4-3B	0.052 (-0.040)	0.057 (-0.035)	0.092
2019-4-12A	<0.020	<0.020	0.004
2019-4-12B	0.080 (0)	0.092 (0.012)	0.080
2019-4-15A	0.035 (-0.009)	0.053 (0.009)	0.044
2019-4-15B	0.154 (-0.014)	0.167 (-0.001)	0.168

Based on the above analysis and combined with your suggestions, I think option 3 is more appropriate. Because option 1 is, after all, an empirical choice, it is difficult to describe quantitatively.

But please note that for the option 3 is chosen. All the FSC estimated result in Tables 2-4, Figure 6, and some description in the original manuscript have been updated.

Meanwhile, I added the following discussion.

Meanwhile, the occurrence times of the peak SO_2 and CO_2 values sometimes have a small deviation that usually corresponds to a few seconds. This is due to two different sensor response times, which leads to three different options for selecting the peak values: 1) the time point of the peak SO_2 value with the CO_2 value at the same time; 2) the time point of the peak CO_2 value with the SO_2 value at the same time; 3) the peak SO_2 and CO_2 values at different time points. Option 3 was selected in this research.

Zhou, F., Pan, S., Chen, W., Ni, X., and An, B.: Monitoring of compliance with fuel sulfur content regulations through unmanned aerial vehicle (UAV) measurements of ship emissions, Atmos. Meas. Tech., 12, 6113–6124, https://doi.org/10.5194/amt-12-6113-2019, 2019.

One of the reviewers pointed out several important issues which could affect the accuracy of the measurements, including cross sensitivity to NO2, the impact of large temperature changes in the exhaust plume and the issues of water vapour and particle contamination of the instruments. Please add a short discussion of these points to the section on uncertainties.

Ok, I have added a short discussion as bellow:

To make it lightweight and convenient, the second-generation pod was only equipped with SO_2 and CO_2 sensors and a simple filter. We did not account for the interference that some factors might have caused, including that due to 1) the cross-sensitivity of the SO_2 sensor to NO_2, 2) the impact of a large temperature change in the exhaust plume, and 3) water vapor and/or particle contamination of the instruments.

In Figure 5, highlight the points used for the FSC computation.

Ok, I have added.

In Figure 6, please indicate by a dotted vertical line the FSC limit of 0.5%.

Ok, I have added.

Quantification of poor measurements: Why don't you use the correlation between SO2 and CO2 time series to determine the quality of a measurement? In my opinion, this should be a good first guess of which measurements to use and which to discard.

Yes, it is indeed a good first guess of which measurements to use and which to discard. I have added the discussion in the manuscript.

Meanwhile, the correlation between the SO_2 and CO_2 time series is a key factor in judging quality. Assuming that the gas is completely mixed, the variation trend of the SO_2 and CO_2 measurements should be the same (although there may be some deviation because the corresponding time of the sensor was not consistent) and can be identified in the peak area.

Comment from the Referee #2：

The authors have improved their study significantly, following the suggestions by the reviewers. I recommend it for publication in AMT.

One short comment: The mixed use of UAV and UAS is sometimes a bit confusing and also not always used in a proper way. The authors should think to skip out one of these very similar acronyms.

OK, after statistics, the rating rate of UAV use was significantly higher. I modified the text to use only the UAV, and the UAS was replace of UAV system.

Other modifications:

On the basis of the research about ship emission monitoring, we have established a provincial-level research center:

Shanghai Engineering Research Center of Ship Exhaust Intelligent Monitoring. Because the name was not determined when this manuscript was submitted, I did not add this institution name. Now, the institution has been formally established.

I apply to add this in the authors' institution information, if the rules allow it.

Finally, thank you for your suggestions, which not only improves the quality of the manuscript, but also makes me more aware of what I need to research in the future.

Monitoring compliance with fuel sulfur content regulations of sailing ships by unmanned aerial vehicle (UAV) measurements of ship emissions in open water

Fan Zhou[1,2], Liwei ~~Hou[2]~~Hou[3], Rui Zhong[1,2], Wei ~~Chen[3]~~Chen[4], Xunpeng ~~Ni[3]~~Ni[4], Shengda Pan[1,2], Ming Zhao[1,4,2,5], Bowen An[1,2]

[1]College of Information Engineering, Shanghai Maritime University, Shanghai 201306, China
[2]Shanghai Engineering Research Center of Ship Exhaust Intelligent Monitoring, Shanghai 201306, China
[2]~~College~~ [3]College of Ocean Science and Engineering, Shanghai Maritime University, Shanghai 201306, China
[3]~~Pudong~~ [4]Pudong Maritime Safety Administration of the People's Republic of China, Shanghai 200137, China
[4]~~Key~~ [5]Key Laboratory of Intelligent Infrared Perception, Chinese Academy of Sciences, Shanghai 200083, China

Correspondence to: Fan Zhou (fanzhou_cv@163.com)

Abstract. Due to technical and cost limitations, the monitoring of emissions from ships sailing in open water within the ship emission control areas (ECAs) is relatively rare. The present study adopts a monitoring method involving an unmanned aerial vehicle (UAV) that takes off from a patrol boat to measure the concentrations of SO_2 and CO_2 within the plumes of sailing ships. Our method aims to provide a low-cost, remote approach for estimating the fuel sulfur content (FSC) of sailing ships in open water, which overcomes the limitations of ground-based and small aircraft methods. The selected monitoring area was the Yangtze River estuary, a domestic ECA with an FSC limit of 0.5% (m/m) implemented by the Chinese government. A total of 27 sailing ships were monitored, ~~14~~ 12 of which were found to have an FSC of > 0.5% (m/m). Moreover, the FSCs of the sailing ships were found to be higher than those of berthing ships in the study area. Based upon the online monitoring results, four of the monitored ships were intercepted by the maritime law enforcement, and fuel samples were collected and analyzed in a laboratory; the results confirmed that all four FSCs were > 0.5% (m/m). Among them, one offending ship was tracked down on July 15, 2019, which was the first time that a sailing ship had been caught for having failed the FSC regulations in China. Overall, the present study provides scientific support for evaluating the effectiveness of ECA policies, and recommends that emissions from sailing ships should be monitored more often in the open water in the future.

1. Introduction

With the rapid development of the shipping industry (UNCTAD, 2017) over the past decades, air pollution caused by ship emissions has received an increasing amount of attention (Eyring et al., 2010; Wan et al., 2016). The pollutant gases emitted by ships not only affect the global climate (Huebert, 1999; Corbet, 2016), but also local air quality and can harm people's health. (Yang et al., 2016; Wang et al., 2019). Shipping accounted for 15%, 13%, and 3% of the annual global anthropogenic emissions of NOx, SOx, and CO_2 from 2007 to 2012, respectively (Smith et al., 2014). In Europe, estimated ship emissions were responsible for 3.0 million tons of NOx, 1.2 million tons of SOx, and 0.2 million tons of fine particulate matter (PM2.5)

in 2011 (Jalkanen et al., 2016). In East Asia, shipping emissions accounted for 16% of global shipping CO_2 in 2013, whereas they only accounted for 4–7% during 2002–2005 (Liu et al., 2016).

To reduce the negative impacts of ship emissions, the International Maritime Organization (IMO) regulates emissions through the International Convention for the Prevention of Pollution from Ships and its Annex VI (MARPOL, 1997). The air-pollution limits for shipping were adopted in 1997, but only came into force in 2005. The global cap for the fuel sulfur content (FSC) of seagoing ships was set at 3.5% (m/m) in 2012, and was reduced to 0.5% (m/m) in 2020. To date, four emission control areas (ECAs) (the Baltic Sea, the North Sea, the United States Caribbean, and the North American and United States Caribbean Sea) have been set up, and the corresponding FSC limit for seagoing ships in these areas was set at 0.1% (m/m) in 2015 (IMO, 2017).

The IMO has not yet set up ECAs in East Asia, which includes the world's ten largest container ports, for example, Shanghai, Ningbo-Zhoushan, and Shenzhen ports. To limit the air pollution caused by ship emissions, the Chinese government established three domestic emission control areas (DECAs) in 2015: the Yangtze River delta, the Pearl River delta, and the Bohai Sea. DECAs was expanded to cover a wider area since 2020, and include most of the coastal ports, the Yangtze River main line, and the Xijiang River main line. The FSC limit for sailing and berthing ships in the DECAs has been set at 0.5% (m/m) since January 1, 2019.

A key problem regarding the implementation of the policy of the ECAs is the question of how to enforce the FSC of ships. Several studies have suggested estimating FSC by measuring ship plumes (Berg et al., 2012; Balzani Lööv et al., 2014). At present, the main method to monitor the emissions of surrounding ships is to place monitoring equipment either on the wharf, shore, port area, or bridge (i.e., ground-based methods) (Alföldy et al., 2013; Pirjola et al., 2013; Beecken et al., 2015; Kattner et al., 2015; Mellqvist et al., 2017a; Cheng et al., 2019; Zhang et al., 2019). Although ground-based methods can provide continuous monitoring, the results obtained depend on the wind speed, wind direction, and the relative position of a ship to the monitoring equipment. Additionally, the boundaries of the ECAs that are designated by the IMO are 200 nautical miles from the coast (Viana et al., 2015); hence, ground-based methods are not able to monitor the fuel that is used on the open sea in ECAs because sailing ships are too far from the shore or bridges.

Therefore, some researchers have used sensors that are carried by small aircrafts to monitor navigating ships within ECAs (Berg et al., 2012; Beecken et al., 2014). However, because this kind of monitoring method is costly, the monitoring of navigating ships is relatively rare. Beecken et al. (2015) observed 434 plumes during ground-based measurements and 32 plumes from a helicopter. Balzani Lööv et al. (2014) took 475 measurements using “sniffing” instruments from ground-based measurements, whereas only 25 measurements were obtained using this method from mobile platforms. In the study undertaken by Mellqvist et al. (2017b), 114 individual ships were measured effectively during 27 flight hours at a cost of approximately 470 Euro per ship, which was for the aircraft cost and did not included the ferry, operator, or instrument rental costs. Therefore, the high cost of flying precludes extensive monitoring of ship emissions.

As a result of the aforementioned factors, there is less monitoring of ships on the open sea in ECAs. This is despite the fact that numerous studies (Pirjola et al., 2014; Kattner et al., 2015; Zhang et al., 2019) have shown that the FSC of ships were

significantly reduced by the implementation of the ECA policy. However, most of these studies did not involve the monitoring of ships on the open water, which could lead to non-representative assessments for the implementation of policies. At the same time, the lack of open sea monitoring results in a blind area for maritime enforcement and is not conducive to the implementation of ship ECA policy by maritime authority. The present study used an unmanned aerial vehicle (UAV) to monitor the FSC of sailing ships on the open sea in the Yangtze River estuary DECA. The method proposed in this study can be used to monitor ship emissions at a comparatively low cost to understand the FSCs of sailing ships in open waters. Although the cost of using patrol boats is not negligible, it is more convenient and cheaper for maritime authorities than using small aircraft~~convenient and lower cost for maritime authorities compared with small aircraft~~.

2 Experimental methods

The research undertaken in the present study forms part of the project "Monitoring and inspecting ship exhaust emissions in the Shanghai free-trade zone" (MISEE). In this project, a~~n unmanned aircraft system (UAS)~~UAS system was designed and developed, and mainly included a pod for measuring the exhaust gas from ships and a UAV to carry the pod. In previous research (Zhou et al., 2019), the plumes of 23 berthing ships were measured using the first-generation pod~~. The~~ , and the deviation of the estimated FSC ~~obtained by the UAS~~ was < 0.03% (m/m) for an FSC of between 0.035% (m/m) and 0.24% (m/m).

In the present monitoring for sailing ships, we developed the second-generation pod by optimizing the structure and layout of the first-generation pod to achieve a lighter weight and smaller volume. A short overview of the instrumentation is provided in Section 2.1. We measured the plumes of 11 berthing ships to verify the accuracy of the second-generation pod, and the plumes of 27 sailing ships to estimate the FSC.

2.1 Instrumentation

The instrumentation~~UAS~~ that was used for monitoring the FSC of sailing ships is shown in Fig 1. The UAV was a MATRICE 600 PRO (SZ DJI Technology Co., Ltd., Shenzhen, China). This type of UAV cannot be used on rainy days or when the wind speed is higher than 8 m/s. The white box installed underneath the UAV in Fig. 1 is the aforementioned second-generation pod for measuring the exhaust gas. When the UAV approaches a ship's plume, the gas pump in the pod draws air using the gas probe. The water vapor, particles, and soot in the gas are subsequently removed by a hose filter valve. The sensors detect the gas and measurement information is sent out by communication modules. The pod has dimensions of 20 cm × 12 cm × 9 cm and weighs 900 g.

The sensors used were able to measure both SO_2 and CO_2, and were purchased from Shenzhen Singoan Electronic Technology Co., Ltd., China. The SO_2 sensor is based on the electrochemical method, and has a measuring range of 0–10 ppm, an accuracy of ± 3% (0.3 ppm), and a response time (T_{90}) of ≤ 30 s. The CO_2 sensor is based on the non-dispersive infrared analyzer method, and has a measuring range of 0–10000 ppm, an accuracy of ± 3% (300 ppm), and a T_{90} of ≤ 30 s. The T_{90} represents the time

taken to reach 90% of the stable response following a full range change in the sample concentration. These sensor characteristics were provided by the instrument manufacturer and were ensured to be within the tolerances by calibration. The zero and full scales are usually calibrated by a standard mixed gas when the equipment is used on a daily basis. The major parameters of the UAV system~~UAS~~ are listed in Table 1.

2.2 Monitoring region

As illustrated in Fig. 2, the monitoring region was the channel of the Yangtze River estuary, near the Waigaoqiao port area to the north of Shanghai. The Yangtse River is the first (third) longest river in China (the world). Shanghai is one of the most prosperous cities in the world, and at the end of 2017 that city had a permanent resident population of approximately 24 million people (Shanghai Municipal Bureau of Statistics, 2017). The Waigaoqiao port area is only 20 km away from the city center, and the air pollution caused by ship emissions directly affects the urban air environment and the health of residents (Wang et al., 2019; Feng et al., 2019). The experimental area of the MISEE project is mainly within the Waigaoqiao port and the Yangtze River estuary.

2.3 Measurement method

During the experiment, the operator took a patrol boat to the channel and then selected a target ship at random. After identifying the target ship for monitoring, the patrol boat would accelerate to a distance to the left or right ahead of the vessel. The patrol boat would then stop and the UAV was operated to takeoff from its deck, and would then fly towards the plume of the target ship and measure the concentrations of SO_2 and CO_2 in the plume (Fig. 3). The distance between the patrol boat and the target ship was a few hundred meters.

During the measurements, the operator adjusted the position of the UAV to ensure that it was in the ship's plume. Real-time measurements of SO_2 and CO_2 were made such that the pod could effectively detect the plume. Generally, it was necessary for the UAV to follow the ship's funnel mouth for approximately 5 minutes, as illustrated in Fig. 4. The target ship continued to move during the measurements; hence, it was followed by the patrol boat in order to avoid the UAV moving too far away from the operator. When the operator was sure that valid data had been collected, the patrol boat stopped and the UAV returned and landed back on the deck of the patrol boat.

2.4 Calculation

The FSC in this study was obtained directly by sampling the gas concentrations in the ship plumes using the UAS. The enhancements of SO_2 and CO_2 in measurements that were affected by exhaust gases were calculated, and the ratio of these SO_2 and CO_2 peaks was used to calculate the FSC (Eqs. 1 and 2). This method has been widely used to calculate the FSC in related studies (Alföldy et al., 2013; Pirjola et al., 2014; Balzani Lööv et al., 2014; Beecken et al., 2014; Beecken et al., 2015; Kattner et al., 2015; Zhou et al., 2019). In the calculation, the molecular weights of carbon and sulfur are 12 g mol^{-1} and 32 g mol^{-1}, respectively, and the carbon mass percent in the fuel is 87 ± 1.5% (Cooper et al., 2003). By assuming that 100% of the

carbon content of the fuel is emitted as CO_2, and sulfur is emitted as SO_2 and other forms, the FSC mass percent can be determined using Eq. (1):

$$FSC[\%] = \frac{S[kg]}{fuel[kg]} = \frac{SO_2[ppm]\cdot A(S)}{CO_2[ppm]\cdot A(C)} \cdot 87[\%] + R = 0.232\frac{\int(SO_{2,peak}-SO_{2,bkg})dt[ppb]}{\int(CO_{2,peak}-CO_{2,bkg})dt[ppm]}[\%] + R = \frac{1}{20}EF[g_{SO_2}/kg_{fuel}] + R, \quad (1)$$

where R represents the sulfur content that is emitted in forms other than SO_2 because preliminary studies have shown that 1–19% of the sulfur in fuel is emitted in other forms, possibly SO_3 or SO_4 (Schlager et al., 2006; Alföldy et al., 2013; Balzani Lööv et al., 2014). EF is the emission factor and bkg is the abbreviation of background. In Eq. (1), if the sensors measuring SO_2 and CO_2 have approximately the same response time and can be set to be synchronized, the peak concentrations of SO_2 and CO_2 can be used to calculate the FSC; otherwise, integrals need to be used. In our research, the sampling rate of the SO_2 and CO_2 sensors was 1 s, and integrals were used because the two sensors could not be completely synchronized.

The continuous measurement data for two typical plumes (2019-4-15B and 2019-3-29A) are exhibited in Fig. 5. The data for plume 2019-4-15B (Fig. 5a) were considered to be of a "good" quality, whereas those for plume 2019-3-29A (Fig. 5c) were considered to be of a "poor" quality. Data were determined to be of a good-quality when obvious, easily distinguished peak values were observed, whereas less obvious peaks that still corresponded to a result were considered as poor-quality data. Meanwhile, the correlation between the SO_2 and CO_2 time series is a key factor in judging quality. Assuming that the gas is completely mixed, the variation trend of the SO_2 and CO_2 measurements should be the same (although there may be some deviation because the corresponding time of the sensor was not consistent) and can be identified in the peak area.

The selection of peak values leads to uncertainty because when the area ratio is selected for the calculation, the starting and ending time points of the area are still associated with substantial uncertainty. Figure 5b and 5d depict the average concentrations of the SO_2 and CO_2 measurements (in Fig. 5a and 5c, respectively) for 10 s periods. The peak value of each average concentration was selected for the calculation. This process is equivalent to selecting the area ratio of SO_2 to CO_2 within 10 s for the calculation, as shown in Eq. (2).

$$FSC[\%] = 0.232\frac{\int(SO_{2,peak}-SO_{2,bkg})dt[ppb]/_{10}}{\int(CO_{2,peak}-CO_{2,bkg})dt[ppm]/_{10}}[\%] + R \approx 0.232\frac{AVG(SO_{2,peak})-AVG(SO_{2,bkg})}{AVG(CO_{2,peak})-AVG(CO_{2,bkg})}[\%], \quad (2)$$

where *AVG* (·) is the calculated function for the average measurement value within 10 s; hence, the data in this study are the average values of measurements in 10 s. When the UAV took off from the patrol boat and flew high into the air, the SO_2 and CO_2 concentrations were relatively low. The background values were obtained at this stage as the minimum SO_2 and CO_2 concentrations. As the UAV flew into the plume, the measured concentrations of SO_2 and CO_2 increased. The obvious, stable maximum values in the observations of the average measurement values should be selected as the peak values. It can be seen that using the average values of measurements within 10 s makes it easier to select the peak values, especially with respect to poor-quality data. However, as there can still be several options for peak values, the data treatment methods reported by Zhou et al. (2019) were incorporated in this study to select the most appropriate peak values. In Fig. 5b, the time point of selected peak values is at 10:19:11. The measurement values from 10:19:57 to 10:20:15 were not used because the CO_2 concentration covered the full range. In Fig. 5d, the time point of the selected peak values is at 10:38:27. The measurement values from

10:39:57 to 10:41:41 were not used because we ruled out data exhibiting either dramatic changes or errors in continuous observations. The details for selecting the peak values are listed in Table 2.

2.5 Uncertainties

In previous research (Zhou et al., 2019), the main uncertainties of UAV measurements were summarized as sensor uncertainty, measurement uncertainty, calculation uncertainty, and exhaust uncertainty. The instrument calibration method, UAV flight procedures, and data treatment methods were designed to reduce these uncertainties. However, some uncertainties remain, as discussed below.

To make it lightweight and convenient, the second-generation pod was only equipped with SO_2 and CO_2 sensors and a simple filter. We did not account for the interference that some factors might have caused, including that due to 1) the cross-sensitivity of the SO_2 sensor to NO_2, 2) the impact of a large temperature change in the exhaust plume, and 3) water vapor and/or particle contamination of the instruments.

The average gas concentration within 10 s was chosen for the FSC calculations; however, this does not mean that 9 s or 11 s could not have been selected. To demonstrate this, a comparison calculation was carried out using both 9 s and 11 s, which showed that these led to very little differences in the results. However, it is necessary to ensure that the gradient of the gas measurements is stable within the sampling time (the interval length of the integral). Moreover, the interval length cannot be too short (e.g., 2 s) or too long (e.g., 20 s). If the time is too short, it is difficult to determine whether the measurements are stable and undisturbed over time. Similarly, if the time is too long, it is also difficult to ensure that all of the measurements in the integral interval are stable and undisturbed. In addition, during the flight of the UAV in this study, the time available for measuring the plume was ~5 minutes. As both the ship and the UAV were moving at this time, it was virtually impossible to ensure that the UAV was flying consistently within the plume and obtaining stable measurements. Accordingly, 10 s is also a relatively appropriate value for the measurement process.

Nevertheless, there is also some uncertainty associated with choosing the peak values. After ruling out the peak values across the full range as well as those corresponding to dramatic changes, the global maximum values were selected as the peak values to calculate the FSC. The maximum values probably correspond to the measurements taken in the center of the ship's plume. At that location, the measurement values were relatively stable, and the probability of interference from other factors was lower. Furthermore, the higher the peak value is, the greater the proportion of exhaust gas is; hence, the impact from the incomplete mixing of the exhaust gas with clean air is relatively small.

In summary, the obvious and stable maximum values are selected as peak values to calculate the FSC. There are, of course, situations where multiple similar peaks can occur simultaneously. In this case, their calculated FSCs may be very similar, and the results obtained by the calculation of the highest peak should have high credibility, for instance, the measurements of plume 2019-4-15B. Meanwhile, the occurrence times of the peak SO_2 and CO_2 values sometimes have a small deviation that usually corresponds to a few seconds. This is due to two different sensor response times, which leads to three different options for selecting the peak values: 1) the time point of the peak SO_2 value with the CO_2 value at the same time; 2) the time point of the

peak CO_2 value with the SO_2 value at the same time; 3) the peak SO_2 and CO_2 values at different time points. Option 3 was selected in this research.

Additional uncertainties were encountered during our monitoring of sailing ships because the UAV was usually hundreds of meters away from the operator. The location of a plume depended primarily on the following three aspects. 1. The position of most plumes with black smoke could be identified through the operator's visual judgment. 2. The real-time image shot by the camera can be used to assist in finding the ship's funnel mouth. 3. In the measurement process, the real-time measured concentration sent to the receiving equipment gradually increased, thus indicating that the UAV was approaching the center of the plume. However, the operator occasionally faced difficulties in accurately determining the ship's plume, which led to failed measurements. We attempted to measure more than 40 ship plumes in open water; however, only 27 of them resulted in good- or poor-quality data, i.e., usable data.

The deviation of the estimated FSC value obtained by the first-generation pod was < 0.03% (m/m) for an FSC level ranging from 0.035% (m/m) to 0.24% (m/m) (Zhou et al., 2019). The second-generation pod was also verified on berthing ships by using this method at a similar FSC level and the accuracy was approximately the same (see Section 3.1). These verifications of the deviation were based on the FSC measurement of berthing ships, which did not exceed the Chinese DECA FSC limit of 0.5% (m/m). However, some of the sailing ships did exceed this limit. It should be noted that the deviations for different FSC levels were not the same. Based on previous studies, the deviation of the FSC obtained from high-sulfur plume should be greater, for example, Van Roy and Scheldeman (2016a, b) estimated relative uncertainties of 20% at a level of 1% (m/m) FSC and 50–100% at 0.1% (m/m) FSC. Therefore, the deviation of sailing ships may > 0.03% (m/m) when the FSC exceeds 0.5% (m/m). Nonetheless, our UAV system~~UAS~~ was still able to accurately detect an FSC that obviously exceeded 0.5% (m/m).

3. Results

3.1 Berthing ships

Before monitoring the sailing ships, we first monitored 11 berthing ships between March and April 2019 in the Waigaoqiao port to verify the accuracy of the second-generation pod. Whilst one person operated the UAV to monitor one of the plumes, two maritime law enforcement officers boarded the corresponding ship to collect a fuel sample. Both processes took approximately 10–20 min. The fuel samples, which are considered to represent the true FSC values, were then sent for chemical analysis in a laboratory. The estimated (UAV) and true FSC values are listed in Table 3 along with the identification number of each plume and the time and serial number. Table 3 shows that the deviation did not generally exceed 0.03% (m/m) for an FSC level of between 0.03% (m/m) and 0.22% (m/m) (except for plume 2019-3-22A and 2019-4-3B). Additionally, when the FSC of a target ship was low, for example, when light diesel fuel was used, the measured SO_2 concentrations were mostly zero. When this occurred, the FSC was generally < 0.02% (m/m), for example, as for plumes 2019-4-3A and 2019-4-12A.

3.2. Sailing ships and comparison with berthing ships

Between March and December 2019, effective monitoring of 27 sailing ships was undertaken using the UAV that took off from the patrol boat (Table 4). The FSC of 23 berthing ships measured by the first-generation monitoring equipment and the FSC of 11 berthing ships (Table 3) measured by the second-generation monitoring equipment in this study were taken as the FSC monitoring results for berthing ships. We compared the distribution of the FSCs of these 34 berthing ships with those of the 27 sailing ships. Figure 6 shows that the FSCs of the sailing ships were considerably higher than those of the berthing ships; the FSC of all 27 sailing ships exceeded 0.1% (m/m) and the FSC of ~~14~~ 12 of these exceeded the Chinese DECA FCS limit of 0.5% (m/m), which included 5 exceedances of ~~2~~1.5% (m/m). The uncertainty in the assessment is not small but the results so far, do not lead to optimism with respect to the FSC used by ships sailing in the area. The reason for this is that although berthing ships are sometimes boarded by maritime law enforcement officers for examination, an effective approach for monitoring the FSC of sailing ships in open water that leads to prosecution by China's maritime authorities has not existed prior to the present study.

According to the monitoring results, law enforcement officers of the Pudong maritime safety administration intercepted four sailing ships for which the UAV FSC results were of a good-quality and all exceeded ~~2~~1.5% (m/m). The officers boarded these ships for inspection on July 15, August 14, August 20, and September 27, 2019, and took fuel samples, which were sent for chemical analysis in a laboratory. The FSC of all four fuels was also found to exceed 0.5% (m/m): 0.534% (m/m), 0.744% (m/m), 0.813% (m/m), and 1.991% (m/m) (in chronological order). The reason that ~~all~~three of these laboratory results did not exceed ~~2~~1.5% (m/m) related to the fact that ships cannot stop immediately in the channel for inspection and have to sail to the anchorage point; when the officers boarded the ships to take samples they found the crew taking various measures to drain the high-sulfur fuel in the main engine fuel oil pipeline. This means that the chemical analysis results of the sampled fuels were obviously lower than those of the UAV monitoring. Nevertheless, the four inspections successfully confirmed that the FSC of the fuels exceeded the standard for sailing ships. The inspection on July 15, 2019, was the first time that a sailing ship's FSC failed to meet Chinese regulations, and this aroused wide concern in the shipping community.

4. Conclusions

In this research, we used a UAV that took off from a patrol boat to monitor emissions from sailing ships in open water. Of the 27 sailing ships that were successfully monitored, ~~14~~ 12 were found to have an FSC that exceeded 0.5% (m/m) and 5 exceeded ~~2~~1.5% (m/m). Based on the monitoring results, law enforcement officers of the Pudong maritime safety administration caught the first case of excessive FSC for a sailing ship and confirmed three other cases. Additionally, the UAV monitoring results demonstrated that the FSC values of sailing ships in the surrounding waters of Waigaoqiao port were higher than those determined for berthing ships in the port. Although the sample size was relatively small, observation of Fig. 6 suggests that the data are still convincing.

Although a global cap on the FSC in marine fuel was set at 3.5% (m/m) in 2012 following the IMO regulation, this was reduced to 0.5% (m/m) in 2020 and has already been implemented in China. According to our monitoring results, the current situation for meeting the 0.5% (m/m) limit is not optimistic. Successful compliance with this regulation by ship owners involves many challenges. We conclude that there is a need for further monitoring data on sailing ships in open water to ascertain the degree of exceedance and work toward compliance.

In addition, there are still some improvements to be made to the UAV system~~UAS~~. 4G transmission is the communication method for detecting information transmission; hence, in locations without a 4G signal (e.g., offshore), the receiving equipment cannot obtain real-time measurement results. Potential solutions include setting-up small base-stations on patrol boats or using satellite transmission. Although carrying an infrared camera on the UAV would make it easier to find the plume, this would require to replace the camera in Fig. 1 with an infrared camera and establish new data communication.

Data availability

Please address requests for data sets and materials to Fan Zhou (fanzhou_cv@163.com).

Author contribution

FZ designed the study and authored the article. FZ and LH analyzed the experimental data. RZ, WC and XN contributed to the experiments. SP contributed to setting instruments. LH, MZ and BA provided constructive comments on this research.

Competing interests

The authors declare that they have no conflict of interest.

Acknowledgements

We thank Megan Anne for English language editing.

Financial support.

This research has been supported by the National Natural Science Foundation of China (grant No. 41701523), the Special Development Fund for China (Shanghai) Pilot Free Trade Zone, the Special Foundation for Intelligent Manufacturing Industry of Shanghai Lin-Gang Area (grant no. ZN2017020325) and Open Project Program of Key Laboratory of Intelligent Infrared Perception, Chinese Academy of Sciences.

References

Alföldy, B., Lööv, J. B., Lagler, F., Mellqvist, J., Berg, N., Beecken, J., Weststrate, H., Duyzer, J., Bencs, L., Horemans, B., Cavalli, F., Putaud, J.-P., Janssens-Maenhout, G., Csordás, A. P., Van Grieken, R., Borowiak, A., and Hjorth, J.: Measurements of air pollution emission factors for marine transportation in SECA, Atmos. Meas. Tech., 6, 1777–1791, https://doi.org/10.5194/amt-6-1777-2013, 2013.

Berg, N., Mellqvist, J., Jalkanen, J.-P., and Balzani, J.: Ship emissions of SO_2 and NO_2: DOAS measurements from airborne platforms, Atmos. Meas. Tech., 5, 1085–1098, https://doi.org/10.5194/amt-5-1085-2012, 2012.

Balzani Lööv, J. M., Alfoldy, B., Gast, L. F. L., Hjorth, J., Lagler, F., Mellqvist, J., Beecken, J., Berg, N., Duyzer, J., Westrate, H., Swart, D. P. J., Berkhout, A. J. C., Jalkanen, J.-P., Prata, A. J., van der Hoff, G. R., and Borowiak, A.: Field test of available methods to measure remotely SOx and NOx emissions from ships, Atmos. Meas. Tech., 7, 2597–2613, https://doi.org/10.5194/amt-7-2597-2014, 2014.

Beecken, J., Mellqvist, J., Salo, K., Ekholm, J., and Jalknen, J.-P.: Airborne emission measurements of SO2, NOx and particles from individual ships using a sniffer technique, Atmos. Meas. Tech., 7, 1957–1968, http://dx.doi.org/10.5194/amt-7-1957-2014, 2014.

Beecken, J., Mellqvist, J., Salo, K., Ekholm, J., Jalkanen, J.-P., Johansson, L., Litvinenko, V., Volodin, K., and Frank-Kamenetsky, D. A.: Emission factors of SO_2, NO_x and particles from ships in Neva Bay from ground-based and helicopter-borne measurements and AIS-based modeling, Atmos. Chem. Phys., 15, 5229–5241, https://doi.org/10.5194/acp-15-5229-2015, 2015.

Cheng, Y., Wang, S., Zhu, J., Guo, Y., Zhang, R., Liu, Y., Zhang, Y., Yu, Q., Ma, W., and Zhou, B.: Surveillance of SO2 and NO2 from ship emissions by MAX-DOAS measurements and implication to compliance of fuel sulfur content, Atmos. Chem. Phys. Discuss., https://doi.org/10.5194/acp-l2019-369, in review, 2019.

Corbett, J.: Shipping emissions in East Asia, Nature Climate Change 6, 983–984, doi:10.1038/nclimate3091, 2016.

Eyring, V., Isaksen, I. S., Berntsen, T., Collins, W. J., Corbett, J. J., Endresen, O., Grainger, R. G., Moldanova, J., Schlager, H., and Stevenson, D. S.: Transport impacts on atmosphere and climate: Shipping, Atmos. Environ., 44, 4735–4771, https://doi.org/10.1016/j.atmosenv.2009.04.059, 2010.

Cooper, D. A.: Exhaust emissions from ships at berth, Atmos. Environ., 37, 3817–3830, https://doi.org/10.1016/s1352-2310(03)00446-1, 2003.

Feng, J., Zhang, Y., Li, S., Mao, J., Patton, A. P., Zhou, Y., Ma, W., Liu, C., Kan, H., Huang, C., An, J., Li, L., Shen, Y., Fu, Q., Wang, X., Liu, J., Wang, S., Ding, D., Cheng, J., Ge, W., Zhu, H., and Walker, K.: The influence of spatiality on shipping emissions, air quality and potential human exposure in the Yangtze River Delta/Shanghai, China, Atmos. Chem. Phys., 19, 6167–6183, https://doi.org/10.5194/acp-19-6167-2019, 2019.

Huebert, B. J.: Sulphur emissions from ships, Nature 400(6746), 713–714. doi:10.1038/23357, 1999.

International Maritime Organization (IMO), Emission Control Areas (ECAs) designated under MARPOL Annex VI.

http://www.imo.org/en/OurWork/Environment/PollutionPrevention/AirPollution/Pages/Emission-Control-Areas-(ECAs)-designated-under-regulation-13-of-MARPOL-Annex-VI-(NOx-emission-control).aspx. Last access 10 December 2019. 2017.

Jalkanen, J.-P., Johansson, L., and Kukkonen, J.: A comprehensive inventory of ship traffic exhaust emissions in the European sea areas in 2011, Atmos. Chem. Phys., 16, 71–84, https://doi.org/10.5194/acp-16-71-2016, 2016.

Kattner, L., Mathieu-Üffing, B., Burrows, J. P., Richter, A., Schmolke, S., Seyler, A., and Wittrock, F.: Monitoring compliance with sulfur content regulations of shipping fuel by in situ measurements of ship emissions, Atmos. Chem. Phys., 15, 10087–10092, doi:10.5194/acp-15-10087-2015, 2015.

Liu, H., Fu, M., Jin, X., Shang, Y., Shindell, D., Faluvegi, G., Shindell, C., and He, K.: Health and climate impacts of ocean-going vessels in East Asia, Nature Climate Change 6, 1037–1041, doi:10.1038/nclimate3083, 2016.

MARPOL: International Convention for the Prevention of Pollution from Ships, 1973 as modified by the Protocol of 1978– Annex VI: Prevention of Air Pollution from Ships, International Maritime Organization (IMO), 1997.

Mellqvist, J., Beecken, J., Conde, V., and Ekholm J.: Surveillance of Sulfur Emissions from Ships in Danish Waters. Chalmers University of Technology, Göteborg, Sweden. December 30, 2017a.

Mellqvist, J., Conde, V., Beecken, J., and Ekholm, J.: Certification of an aircraft and airborne surveillance of fuel sulfur content in ships at the SECA border, CompMon (https://compmon.eu/, last access: 6 November 2018), 2017b.

Pirjola, L., Pajunoja, A., Walden, J., Jalkanen, J.-P., Rönkkö, T., Kousa, A., and Koskentalo, T.: Mobile measurements of ship emissions in two harbour areas in Finland, Atmospheric Measurement Techniques 6(4), 7149–7184. doi:10.5194/amtd-6-7149-2013, 2013.

Schlager, H., Baumann, R., Lichtenstern, M., Petzold, A., Arnold, F., Speidel, M., Gurk, C., and Fischer, H.: Aircraft-based Trace Gas Measurements in a Primary European Ship Corridor, Proceedings TAC-Conference, 26–29 June, Oxford, 83–88, 2006.

Shanghai Municipal Bureau of Statistics. The statistic communique of Shanghai on the 2017 national economy and social development, 2017.

Smith, T. W. P. et al. Third IMO Greenhouse Gas Study 2014. International Maritime Organization, 2014.

UNCTAD: World seaborne trade by types of cargo and by group of economies, annual, United Nations Conference on Trade and Development, available at: https://unctadstat.unctad.org/wds/TableViewer/tableView.aspx?ReportId=32363, last access: 5 March, 2017.

Van Roy, W. and Scheldeman, K.: Results MARPOL Annex VI Monitoring Report Belgian Sniffer Campaign 2016, CompMon (https://compmon.eu/, last access: 6 November 2018), 2016a.

Van Roy, W. and Scheldeman, K.: Best Practices Airborne MARPOL Annex VI Monitoring, CompMon (https://compmon.eu/,last access: 6 November 2018), 2016b.

Viana, M., Fann, N., Tobías, A., Querol, X., Rojas-Rueda, D., Plaza, A., Aynos, G., Conde, J., Fernaìndez, L., and Fernández, C.: Environmental and health benefits from designating the marmara sea and the Turkish straits as an emission control area (ECA), Environ. Sci. Technol., 49, 3304–3313, https://doi.org/10.1021/es5049946, 2015.

Wan, Z., Zhu, M., Chen, S., and Sperling, D.: Pollution: Three steps to a green shipping industry, Nature 530, 275–277, doi:10.1038/530275a, 2016.

Wang, X., Shen, Y., Lin, Y., Pan, J., Zhang, Y., Louie, P. K. K., Li, M., and Fu, Q.: Atmospheric pollution from ships and its impact on local air quality at a port site in Shanghai, Atmos. Chem. Phys., 19(9), 6315–6330. doi:10.5194/acp-19-6315-2019, 2019.

Yang, M., Bell, T. G., Hopkins, F. E., and Smyth, T. J.: Attribution of atmospheric sulfur dioxide over the English Channel to dimethyl sulfide and changing ship emissions, Atmos. Chem. Phys., 16, 4771–4783, https://doi.org/10.5194/acp-16-4771-2016, 2016.

Zhang, Y., Deng, F., Man, H., Fu, M., Lv, Z., Xiao, Q., Jin, X., Liu, S., He, K., and Liu, H.: Compliance and port air quality features with respect to ship fuel switching regulation: a field observation campaign, SEISO-Bohai, Atmos. Chem. Phys., 19, 4899–4916, https://doi.org/10.5194/acp-19-4899-2019, 2019.

Zhou, F., Pan, S., Chen, W., Ni, X., and An, B.: Monitoring of compliance with fuel sulfur content regulations through unmanned aerial vehicle (UAV) measurements of ship emissions, Atmos. Meas. Tech., 12, 6113–6124, https://doi.org/10.5194/amt-12-6113-2019, 2019.

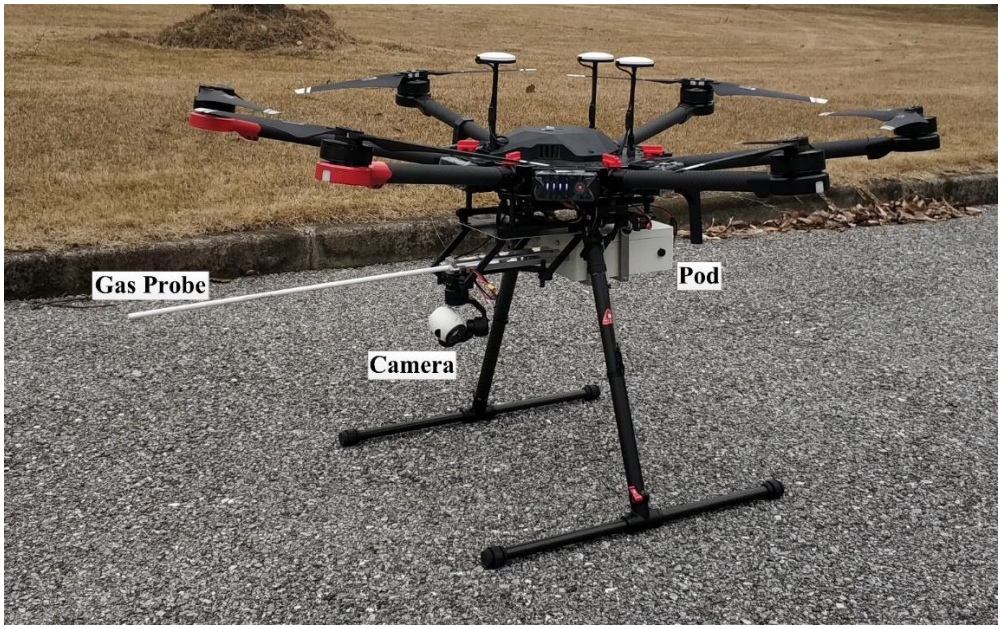

Figure 1. Image of the unmanned aircraft system. A gas probe, camera, and pod are installed under the unmanned aerial vehicle (UAV). The gas probe is used to collect the ship's exhaust gas, and the camera is used to assist in finding the ship's funnel mouth during flight. The pod is used to carry a gas pump, gas circuit, filter, small motor, sensors for SO_2 and CO_2, and communication modules.

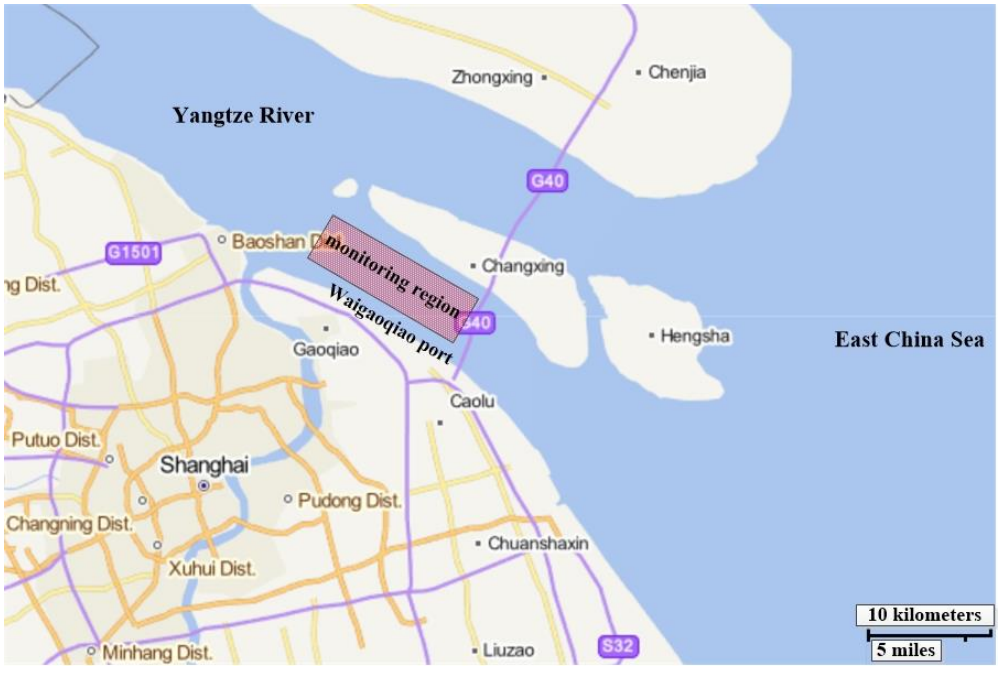

Figure 2. Monitoring regions in the channel of Yangtze River estuary, which belong to the DECAs of China. This area is to the north of Shanghai, on the southwest side of Changxing Island. The distance between the two sides is ~6–7 km. Ships leave the Yangtze

River and sail into the East China Sea through this channel. Map data: @MapWorld (http://www.tianditu.gov.cn, last access: 5 March 2020).

Figure 3. Operator controlling the takeoff of the UAV from a patrol boat.

Figure 4. UAV (marked by a red circle) monitoring a ship's emissions in the open sea. The enlarged UAV is shown in the top left corner. This picture was captured by another UAV.

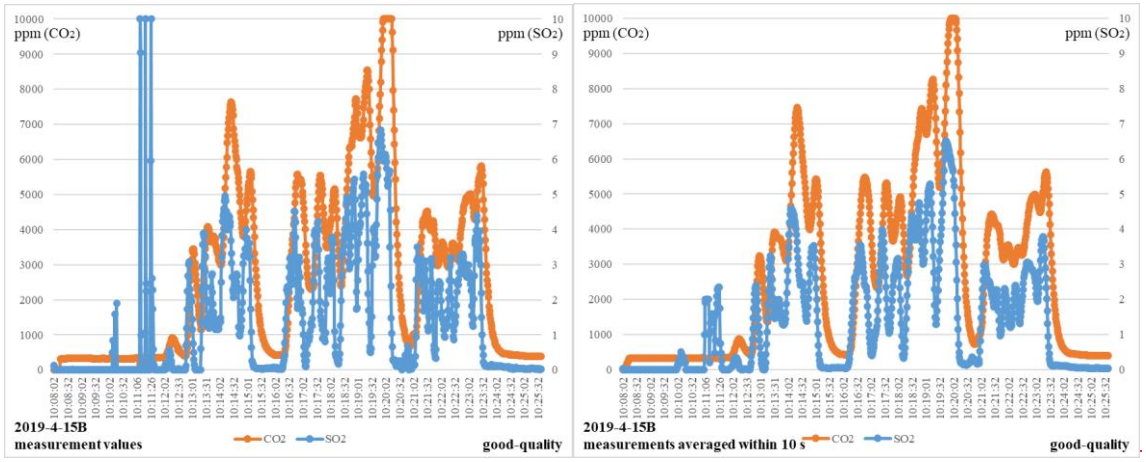

(a) (b)

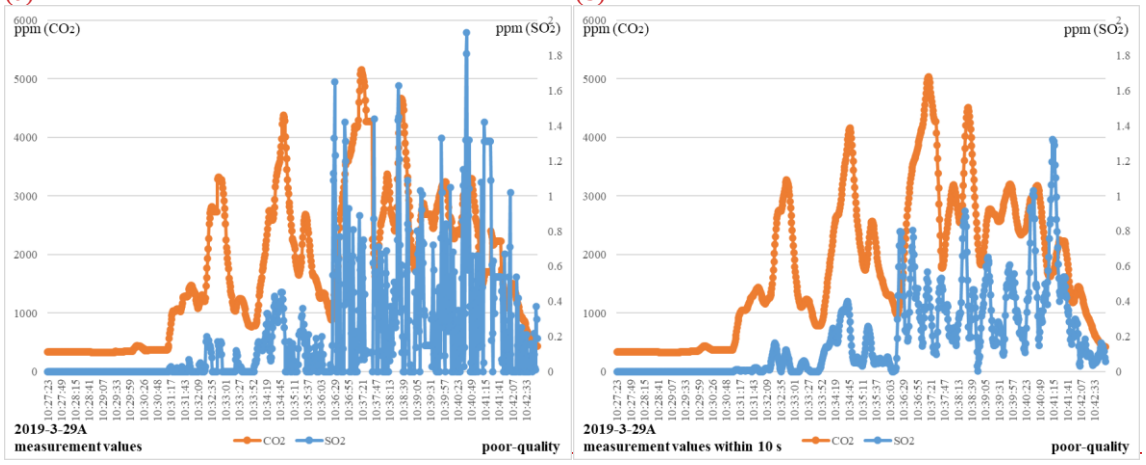

(c) (d)

Figure 5. Typical measurement data for SO_2 and CO_2 concentrations, and their corresponding average values within 10 s. (a) and (b) good-quality data from plume ID 2019-4-15B. (c) and (d) poor-quality data from plume ID 2019-3-29A. There are some errors in the measurements from 10:11:06 to 10:12:02 in (a), which may have been caused by sensor uncertainty. These data were ruled out and did not affect the calculation results.

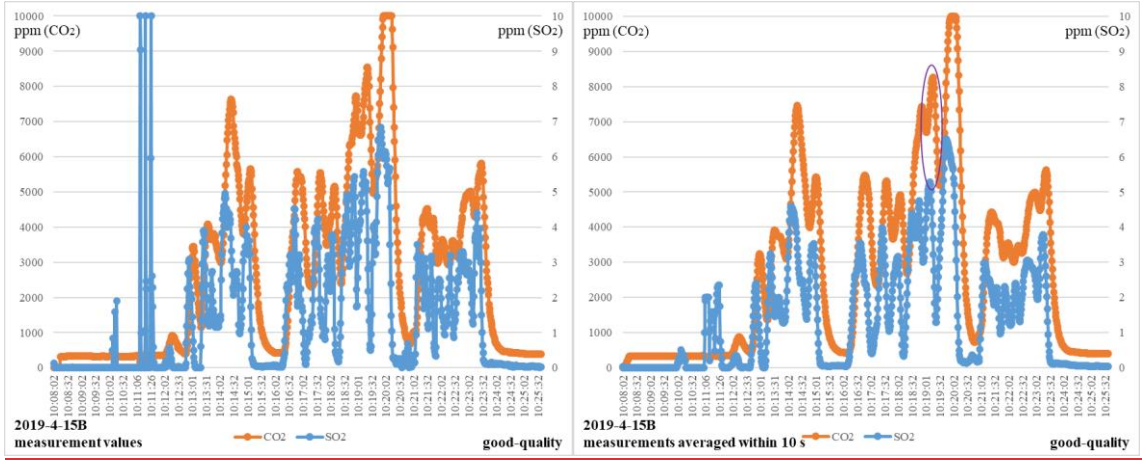

(a) (b)

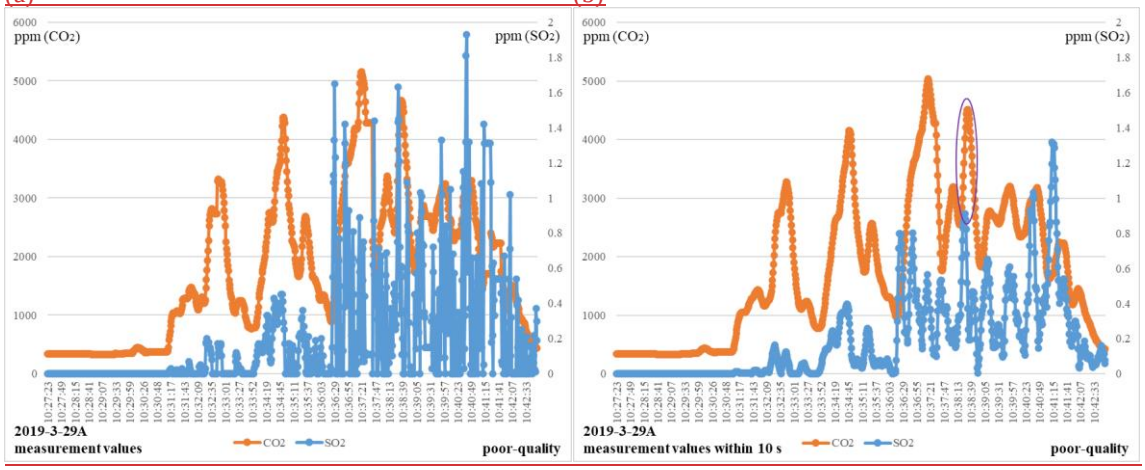

(c) (d)

Figure 5. Typical measurement data for SO_2 and CO_2 concentrations, and their corresponding average values within 10 s. (a) and (b) good-quality data from plume ID 2019-4-15B. (c) and (d) poor-quality data from plume ID 2019-3-29A. There are some errors in the measurements from 10:11:06 to 10:12:02 in (a), which may have been caused by sensor uncertainty. These data were ruled out and did not affect the calculation results. After selection, the peak values are circled in purple.

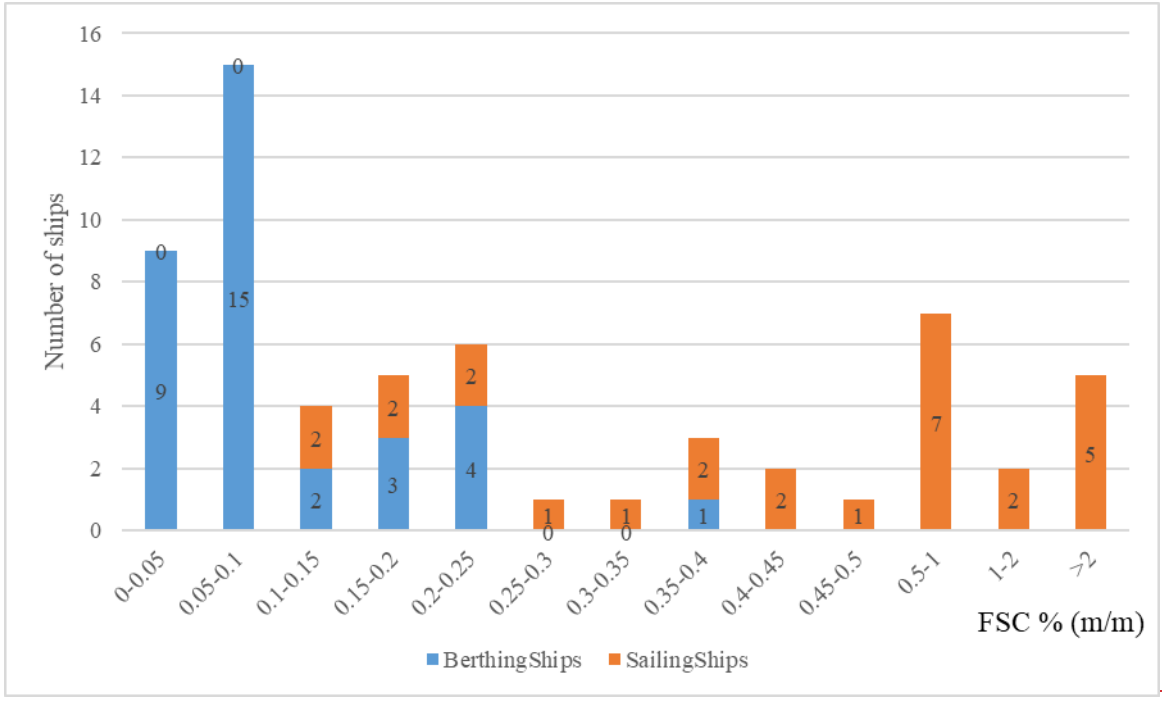

~~**Figure 6. Comparison between the monitoring results of berthing ships and sailing ships.**~~

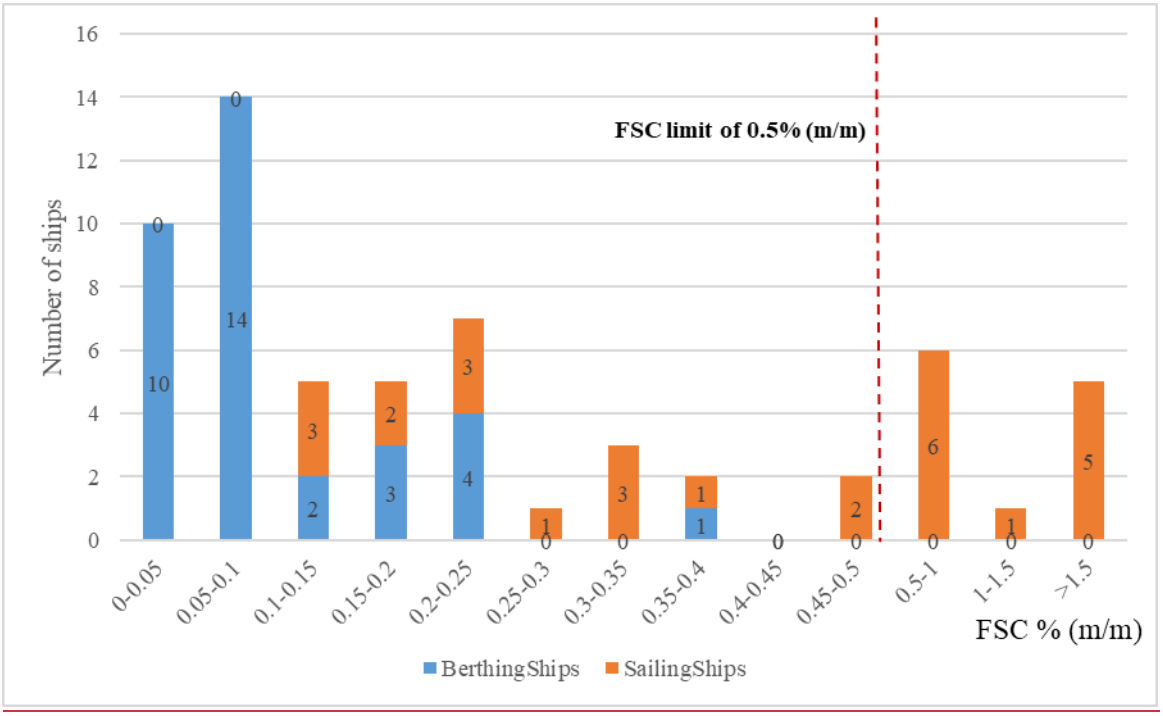

Figure 6. Comparison between the monitoring results of berthing ships and sailing ships.

510

Table 1: Parameters of the UAV system.~~UAS~~

	Parameter	Value
UAV	Symmetrical motor wheelbase	1133 mm
	Size	1668 mm × 1518 mm × 727 mm
	Weight	9.5 kg
	Recommended maximum take-off weight	15.5 kg
	Hovering accuracy(P-GPS)	Vertical: ±0.5 m, Horizontal: ±1.5 m
	Maximum rotational angular velocity	Pitch axis: 300°/s, Heading axis: 150°/s
	Maximum pitch Angle	25°
	Maximum rising speed	5 m/s
	Maximum rate of descent	3 m/s
	Maximum sustained wind speed	8 m/s
	Maximum horizontal flight speed	65 km/h (no wind environment)
	Hover time	Non-loaded: 32 min; load 6 kg: 16 min
SO_2 sensor	Type	SGA-700A-SO2
	Principle	Electrochemistry
	Measuring range	0–10 ppm
	Diameter and height	33.5 mm; 31 mm
	Weight	30 g
	Accuracy	≤ ±3 % (0.3 ppm)
	Linear error	≤ ±2 % (0.2 ppm)
	Repeatability	≤ ±2 % (0.2 ppm)
	Power consumption	≤ 50 mA
	Response time (T_{90})	≤ 30 s
CO_2 sensor	Type	SGA-700A-CO2
	Principle	Non-Dispersive InfraRed
	Measuring range	0–10000 ppm
	Diameter and height	33.5 mm; 31 mm
	Weight	30 g
	Accuracy	≤ ±3 % (300 ppm)
	Linear error	≤ ±2 % (200 ppm)
	Repeatability	≤ ±2 % (200 ppm)
	Power Consumption	≤ 100 mA
	Response time (T_{90})	≤ 30 s

Table 2: All peak values and their corresponding FSC results. The background values of plume 2019-4-15B were 0 ppm and 310 ppm for SO_2 and CO_2, respectively. The background values of plume 2019-3-29A were 0 ppm and 329 ppm for SO_2 and CO_2, respectively. The remarks indicate the reason for choosing or not choosing the peak. It can be seen that the peak value of plume 2019-4-15B was more obvious and that the results obtained by multiple alternative peaks were similar. The peak of plume 2019-3-29A was less obvious and there were fewer alternative peaks. This was also the basis for distinguishing data as being of a "good"/"poor" quality. The FSC result of selected peak values are marked as "√".

Plume ID	Time point	Peak value of SO_2 and CO_2 (ppm)	Estimated value of FSC (% (m/m))	True value of FSC (% (m/m))	Remark
2019-4-15B	10:12:52	2.406, 2020	0.326	0.168	Reject; less obvious peak values
	10:13.23	3.235, 2372	0.364		
	10:14.07	4.594, 4665	0.245		Non-maximum peaks of alternative peak values
	10:14.57	3.529, 4872	0.179		
	10:16.39	3.549, 4444	0.199		
	10:17:27	3.989, 3911	0.257		
	10:18:01	3.159, 4607	0.171		
	10:18:47	4.757, 6895	0.168		
	10:19:11	5.287, 7634	0.167 (√)		Maximum peak of the alternative peak value
	10:19:46	6.515, 8100	0.194		Reject; measurements exceeded the range
2019-3-29A	10:34:41	0.399, 3880	0.026	0.035	Reject, less obvious peak values
	10:35:19	0.258, 2011	0.036		Non-maximum peaks of the alternative peak values
	10:37:15	0.567, 4994	0.028		Reject; less obvious peak values
	10:38:27	0.913, 4022	0.057 (√)		Maximum peak of the alternative peak value
	10:40:37	1.031, 2996	0.090		Reject; error in the measurement data
	10:41:13	1.321, 1700	0.224		

Table 2: All peak values and their corresponding FSC results. The background values of plume 2019-4-15B were 0 ppm and 310 ppm for SO_2 and CO_2, respectively. The background values of plume 2019-3-29A were 0 ppm and 329 ppm for SO_2 and CO_2, respectively. The remarks indicate the reason for choosing or not choosing the peak. It can be seen that the peak value of plume 2019-4-15B was more obvious and that the results obtained by multiple alternative peaks were similar. The peak of plume 2019-3-29A was less obvious and there were fewer alternative peaks. This was also the basis for distinguishing data as being of a "good"/"poor" quality. The FSC result of selected peak values are marked as "√". As the sensor response time was inconsistent, only the SO_2 peak time points are listed (the CO_2 peak time points had a delay of several seconds).

Plume ID	Time point of the SO_2 peak	Peak value of SO_2 and CO_2 (ppm)	Estimated value of FSC (% (m/m))	True value of FSC (% (m/m))	Remark
2019-4-15B	10:12:52	2.406, 3247	0.190	0.168	Reject; less obvious peak values
	10.13.23	3.235, 3913	0.208		
	10.14.07	4.594, 7461	0.149		Non-maximum peaks of alternative peak values
	10.14.57	3.529, 5429	0.160		
	10.16.39	3.549, 5475	0.159		
	10:17:27	3.989, 5322	0.185		
	10:18:01	3.159, 4923	0.159		
	10:18:47	4.757, 7430	0.155		
	10:19:11	5.287, 8276	0.154 (√)		Maximum peak of the alternative peak value
	10:19:46	6.515, 10000	0.156		Reject; measurements exceeded the range
2019-3-29A	10:34:41	0.399, 4160	0.024	0.035	Reject, less obvious peak values
	10:35:19	0.258, 2570	0.027		Non-maximum peaks of the alternative peak values
	10:37:15	0.567, 5036	0.028		Reject; less obvious peak values
	10:38:27	0.913, 4517	0.051 (√)		Maximum peak of the alternative peak value
	10:40:37	1.031, 3179	0.084		Reject; error in the measurement data
	10:41:13	1.321, 2254	0.159		

Table 3: Comparison and verification of the estimated (UAV) and true (sampled fuel) values of the FSC from 11 berthing ships.

ID	Estimated value of FSC (% (m/m))	True value of FSC (% (m/m))	Deviation (% (m/m))	Quality
2019-3-18A	0.217	0.222	-0.005	Good
2019-3-22A	0.069	0.099	-0.030	Good
2019-3-22B	0.046	0.042	0.004	Good
2019-3-29A	0.057	0.035	0.022	Poor
2019-4-1A	0.090	0.079	0.011	Good
2019-4-3A	<0.020	0.013	N	Poor
2019-4-3B	0.057	0.092	-0.035	Good
2019-4-12A	<0.020	0.004	N	Poor
2019-4-12B	0.092	0.080	0.012	Good
2019-4-15A	0.053	0.044	0.009	Good
2019-4-15B	0.167	0.168	-0.001	Good

Table 4: Estimated (UAV) values of the FSC from 27 sailing ships. "*" indicates that the ship was boarded by the maritime authority for inspection, and the value shown in parentheses is the result of the chemical examination of the fuel.

ID	Estimated value of FSC (% (m/m))	Quality	ID	Estimated value of FSC (% (m/m))	Quality
2019-7-12A	0.781	Good	2019-8-22A	0.186	Good
2019-7-15A	0.646	Good	2019-8-22B	0.385	Poor
2019-7-15B*	3.369 (0.534)	Good	2019-8-22C	0.415	Good
2019-7-25A	0.580	Good	2019-8-22D	0.112	Poor
2019-7-25B	0.675	Good	2019-8-22E	0.104	Good
2019-8-14A*	2.672 (0.744)	Good	2019-8-22F	0.239	Poor
2019-8-15A	0.382	Good	2019-9-17A	0.202	Good
2019-8-15B	0.694	Poor	2019-9-17B	0.628	Poor
2019-8-16A	0.175	Poor	2019-9-27A	0.419	Poor
2019-8-16B	0.267	Poor	2019-9-27B*	3.450 (1.991)	Good
2019-8-16C	1.127	Good	2019-10-9A	2.116	Poor
2019-8-16D	0.700	Poor	2019-10-17A	0.481	Good
2019-8-20A	1.508	Poor	2019-10-24A	0.326	Good
2019-8-20B*	4.091 (0.813)	Good			

Table 3: Comparison and verification of the estimated (UAV) and true (sampled fuel) values of the FSC from 11 berthing ships.

ID	Estimated value of FSC (% (m/m))	True value of FSC (% (m/m))	Deviation (% (m/m))	Quality
2019-3-18A	0.207	0.222	-0.015	Good
2019-3-22A	0.062	0.099	-0.037	Good
2019-3-22B	0.046	0.042	0.004	Good
2019-3-29A	0.051	0.035	0.016	Poor
2019-4-1A	0.064	0.079	-0.015	Good
2019-4-3A	<0.020	0.013	N	Poor
2019-4-3B	0.052	0.092	-0.040	Good
2019-4-12A	<0.020	0.004	N	Poor
2019-4-12B	0.080	0.080	0	Good
2019-4-15A	0.035	0.044	-0.009	Good
2019-4-15B	0.154	0.168	-0.014	Good

Table 4: Estimated (UAV) values of the FSC from 27 sailing ships. "*" indicates that the ship was boarded by the maritime authority for inspection, and the value shown in parentheses is the result of the chemical examination of the fuel.

ID	Estimated value of FSC (% (m/m))	Quality	ID	Estimated value of FSC (% (m/m))	Quality
2019-7-12A	0.634	Good	2019-8-22A	0.178	Good
2019-7-15A	0.482	Good	2019-8-22B	0.328	Poor
2019-7-15B*	1.563 (0.534)	Good	2019-8-22C	0.376	Good
2019-7-25A	0.523	Good	2019-8-22D	0.102	Poor
2019-7-25B	0.521	Good	2019-8-22E	0.104	Good
2019-8-14A*	2.231 (0.744)	Good	2019-8-22F	0.232	Poor
2019-8-15A	0.305	Good	2019-9-17A	0.196	Good
2019-8-15B	0.694	Poor	2019-9-17B	0.567	Poor
2019-8-16A	0.137	Poor	2019-9-27A	0.278	Poor
2019-8-16B	0.202	Poor	2019-9-27B*	3.449 (1.991)	Good
2019-8-16C	0.536	Good	2019-10-9A	2.004	Poor
2019-8-16D	0.451	Poor	2019-10-17A	0.305	Good
2019-8-20A	1.022	Poor	2019-10-24A	0.229	Good
2019-8-20B*	3.381 (0.813)	Good			